Archaeometry **43**, 1 (2001) 117–129. Printed in Great Britain

THE USE OF SMALL-ANGLE X-RAY DIFFRACTION STUDIES FOR THE ANALYSIS OF STRUCTURAL FEATURES IN ARCHAEOLOGICAL SAMPLES*

T. J. WESS,[1] M. DRAKOPOULOS,[2] A. SNIGIREV,[2] J. WOUTERS,[3] O. PARIS,[4] P. FRATZL,[4] M. COLLINS,[5] J. HILLER[5] and K. NIELSEN[6]

[1]*Department of Biological Sciences, University of Stirling, Stirling, Scotland, UK*
[2]*ESRF, 6 rue Jules Horowitz, 38043 Grenoble, France*
[3]*Royal Institute for Artistic Heritage, Jubelpark 1. 1000 Brussels, Belgium*
[4]*Erich Schmid Institute of Materials Science, Austrian Academy of Sciences & Metal Physics Institute, University of Leoben, Jahnstr. 12, A-8700 Leoben, Austria*
[5]*NRG Unit, Fossil Fuels & Environmental Geochemistry, Drummond Building, University of Newcastle-upon-Tyne, England, UK*
[6]*Department of Chemistry, Technical University Denmark, 2800, Lyngby, Denmark*

X-ray diffraction or scattering analysis provides a powerful non-destructive technique capable of providing important information about the state of archaeological samples in the nanometer length scale. Small-angle diffraction facilities are usually found at synchrotron sources, although the potential of a laboratory source is also described. Specific examples of analysis using X-ray diffraction of historic parchment, archaeological bone, a Central Mexico style pictograph and microdiffraction of calcified tissues are used to show the scope and versatility of the technique. Diffraction data is capable of giving fundamental structural information as well as quantifying the remodelling of structures influenced by environmental factors.

KEYWORDS: SMALL-ANGLE SCATTERING, PARCHMENT, BONE, DIAGENESIS, POWDER DIFFRACTION, MOLECULAR STRUCTURE

INTRODUCTION

One of the main factors concerning archaeological and historical materials is their unique properties and their often irreplaceable nature. Analysis of a sample is required to extract the maximum amount of information: however, the techniques used for the analysis of the sample, such as amino acid analysis or carbon dating, can be destructive. Non-destructive techniques, or techniques that use very small samples on a micron scale, are preferred, especially if they can access similar information to techniques that require loss of sample integrity. X-ray diffraction can be used to examine the internal structural features of matter, and in some circumstances, can be used in a non-destructive manner, especially on samples less than 1 mm in thickness, but this also depends on the sample density.

Background to X-ray scattering

Many materials contain long-range order, or consist of particles that have a size that is readily investigated by X-ray scattering: the ability of a sample to diffract or scatter principally depends on the ordering of the material. All matter will scatter X-rays: fluctuations in the electron density

* Received 10 April 2000, accepted 5 July 2000.

of the sample, such as at the interface between molecules, give rise to a characteristic scattering pattern. The interactions that contribute to the scattering process correspond to length scales from the submicron scale to the Ångstrom region. This level of detail is submicroscopic and gives information about the organization of atoms and molecules within a sample. In order to understand fully the results from X-ray diffraction or scattering analysis, it is beneficial to understand the interactions between X-rays and matter. The theory is beyond the scope of this paper, but is covered in detail in books by Vainshtein (1966), Guinier (1963), Fraser and MacRae (1973) and Hukins (1981). A review of small-angle X-ray scattering can be found in Perkins *et al.* (1998). This paper, however, is aimed at the non-specialist user who may see the potential benefits of X-ray scattering as part of sample characterization.

The difference between X-ray scattering and diffraction depends on the organization of matter within the object being analysed. A simple way to distinguish between the processes is to consider whether a level of structural organization within the sample involves the regular spacing of atomic or molecular species. Where molecular species have a recognizable ordering that results from regular packing, this leads to coherent accumulation of the scattering signal—this is diffraction. This results in discrete peaks of X-ray intensity that can be observed at specific angles deflected from the sample. When the species have no recognizable spatial relationship with each other, the scattering from the individual species does not add together coherently and the scattering is not sampled at discrete intervals but extends over sectors of the scattering angle. The differences between a sample that exhibits scattering and one that exhibits diffraction at small angles is shown in the figures that accompany this paper. The position of diffraction peaks, their intensity and their angular distribution can provide information about the structure within a sample. The shape and radial distribution of the observed scattering can also be used to infer particle size, density and surface area.

Synchrotron radiation and small-angle scattering

Synchrotron radiation sources provide high-brilliance and highly parallel X-ray beams that can produce images from samples that contain poor density contrast, and where data collection on a conventional source may take days. In the case of small-angle experiments, the main beam divergence has to be minimized, so that the scattering from the sample can be distinguished from the main beam. Sample-to-detector distances of up to 10 m can be used to observe the long-range molecular organization of a sample. At beamline 2.1 at the CCLRC Daresbury synchrotron (Cheshire, UK; see Towns-Andrews *et al.* 1989), these camera lengths can be attained with a corresponding small spot size ($500\,\mu\text{m} \times 2000\,\mu\text{m}$) at the sample and a well focused diffraction image at the detector. The detector systems are also important in being sensitive yet having a large dynamic range; for details, see Lewis (1994). The process of diffraction allows the overall structure of a statistically significant population of particles, crystal or fibres to be examined at one time. Care must be taken to assess whether the ionization and free radical damaged caused by X-rays is significant: this is especially important in the case of samples with a high moisture content. In the case of parchment, a large number of samples (up to 200) can be analysed during one day of synchrotron beam time. A schematic diagram of the diffraction layout is shown in Figure 1.

Advances in X-ray optics complement synchrotron radiation in producing X-ray beams that are focused on to a micron-sized spot at the sample, therefore allowing detailed textural analysis of structural features. A micro-beam facility for Small-Angle X-Ray Scattering (micro-SAXS) has been developed at beamline ID22 of the European Synchrotron Research Facility.

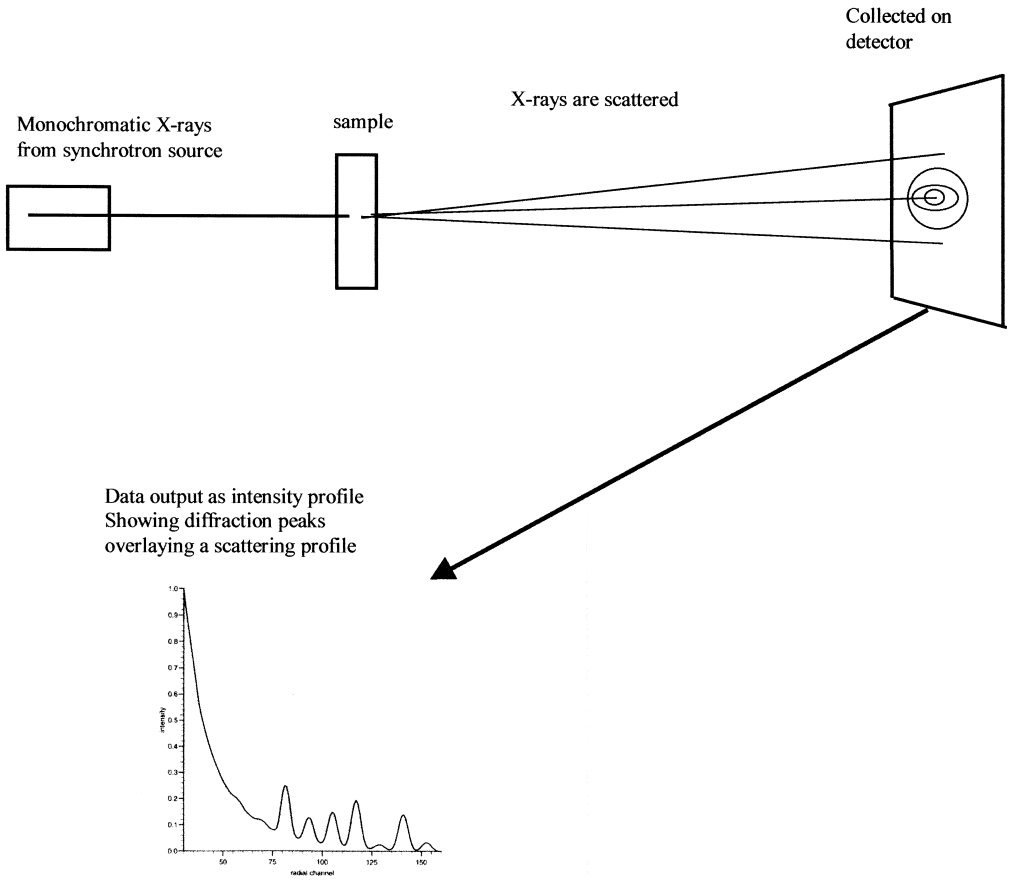

Figure 1 *A schematic diagram of synchrotron small-angle scattering. The highly parallel X-ray beam is defined by optical elements and finally by a series of horizontal and vertical slits. The nature of small-angle diffraction means that the scattered X-rays are close to the main X-ray beam and long camera lengths are used to help resolve the two. In order to sustain the intensity of the X-rays, the diffracted and main beam pass through an evacuated 'camera' that minimizes the air path between the sample and the detector.*

The low divergent micro-beam is prepared with a Fresnel-zone plate, attaining a focal spot size of 1 μm vertically by 6 μm horizontally and a flux of 5×10^{10} photons per second at 10 keV. A collimator system after the zone plate is used to reduce the background intensity to negligible values, although limiting accessible q-space currently to a minimum value of 0.09 nm^{-1}. The ultimate resolution in q-space is determined by the beam divergence after the zone plate and is approximately 0.005 nm^{-1}. However, with better collimator systems an higher resolution than the current value can be achieved. The scattered intensity is recorded using a CCD detector with a coupled fibre optic taper and a large dynamic range of nearly 16 bit.

Some samples that are of special interest in archaeometry, such as bone, scatter X-rays strongly and essential information about the crystal habit can be obtained with conventional X-ray laboratory sources. These data can be combined with more detailed studies made with microfocal optics at synchrotron sources.

THREE EXAMPLES OF SAMPLE ANALYSIS BY X-RAY DIFFRACTION

The potential use of X-ray diffraction and scattering techniques is probably best described by giving examples of their application and analysis of the data obtained. Below, four examples of diffraction techniques are described; these range from small-angle scattering studies of archaeological bone using a conventional laboratory X-ray source to microfocus diffraction of a Central Mexico style approximately 16th century pictograph sample at a third-generation synchrotron.

Analysis of historic parchments

Historic parchment contains much of the European written heritage of the Middle Ages. One of the principal concerns is the contemporary deterioration of parchments as a result of pollution and microbial action. The major effects of pollution are believed to be through oxidative damage and the physical basis of the deterioration is not well resolved. Small-angle X-ray scattering has been used as a technique to analyse the changes that have occurred in over 30 historical parchment samples, as part of a European project on the development of non-destructive and complementary microdiffraction techniques.

Background The axial structure of fibrillar collagen is well documented. Studies using X-ray diffraction, neutron diffraction and electron microscopy have provided most of the data that have allowed relatively detailed maps of the molecular packing to be produced. When associated in fibrils, 300 nm long collagen molecules have a molecular alignment based on relative staggers of 67 nm repeats. The staggered molecules result in a projected structure that contains the characteristic gap/overlap feature based on a 67 nm periodicity (Wess *et al.* 1998).

In the vast majority of cases, the studies have been made on molecular structures that are maintained as close as possible to the native structural state of tissues such as skin and tendon. However, in the analysis of parchment the sample is dry and this has a number of effects on the diffraction data before any effects of deterioration are considered:

(1) The periodicity of the axial repeat is shortened from 67 nm to approximately 64 nm.
(2) The intensity of Bragg reflections changes radically, indicating changes in electron density.
(3) The number of diffraction peaks is curtailed after only 15 diffraction orders in the dry state and indicates a relatively high degree of static disorder in the sample.

These features can be quantified by X-ray diffraction, and the relevance to ageing and decay of parchment samples then assessed by judging further changes observed in the quality of diffraction data.

Data were collected at beamline 2.1 of the CCLRC Daresbury Laboratory. A 4.5 m camera allowed adequate resolution of the first 15 individual axial Bragg peaks, which correspond to the meridional series that can be observed with dried collagen-based tissues. The diffracted X-rays were detected with a two-dimensional gas-filled detector that has a very large dynamic range. Data were corrected for a detector response in order to normalize each pixel of the detector. Background diffraction images were removed in order to eliminate camera-dependent diffraction effects. Examples of typical diffraction patterns are shown in Figure 2. The diffraction peaks corresponding to the axial electron density repeat of collagen appear as a series or arcs, and in some cases as concentric circles. This is due to the fact that the collagen fibrils are distributed as random orientations in the plane of the parchment (writing surface). However, the fibrils are more confined in the direction perpendicular to the plane of the parchment; such a distribution is known as a felt.

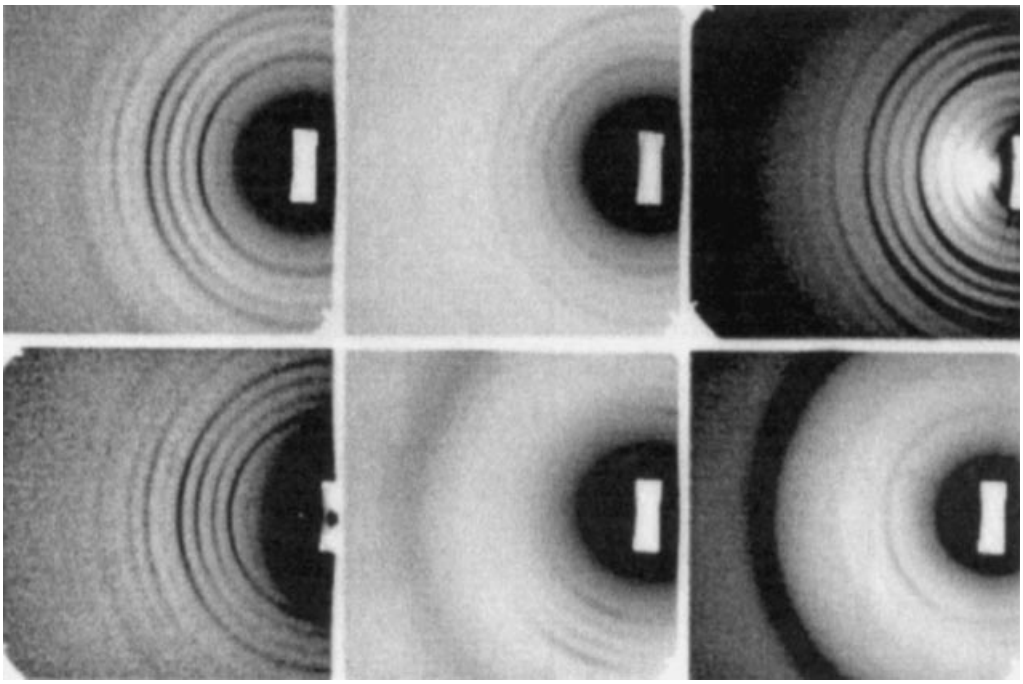

Figure 2 *Diffraction of historic parchments. The variety of X-ray diffraction profiles that can be obtained from historic parchments (c. 16th–18th century, obtained from the Royal Danish archive is shown here. The strong diffraction peaks resulting from the natural contrast within a collagen fibril sample are superimposed on a highly sloping sample-derived background. Some samples exhibit a strong crystalline lipid diffraction ring that can be seen at the edge of the detector. The intensity of the diffraction profiles is used to assess the state of deterioration of the collagen fibrils within the parchment samples.*

Data analysis The diffraction data obtained from the detector was converted to a linear intensity distribution over a fixed angular range that corresponded to the optimal fibril orientation in the sample. In order to collect a well spaced diffraction series, the detector was offset to the diffraction origin and therefore it was not possible to collect information from all angles subtended by a truly isotropic sample. Each parchment was aligned to record the major fibre orientation and a subsequent orthogonal orientation was recorded for each sample in order to collect at least 180° of each diffraction arc. The linear profile was corrected for the Lorenz effect due to sample diffraction smearing with a increased diffraction angle (2θ). This was applied as a simple linear function proportional to the position of the diffraction order. Each image was transposed into a polar co-ordinate system, which converts the arcs of diffraction into straight lines: the image was then integrated over a fixed range of θ to obtain each density profile. No correction was made for the angular distribution in the plane orthogonal to the plane containing the felt-like distribution of the collagen fibrils.

The variety of samples collected produced a number of different diffraction profiles: however, all samples analysed at the SRS Daresbury contained characteristic and consistent features. In almost all cases, the molecular spacing of the axial structure was around 64 nm, with only a small number of samples that deviated significantly from this value. The diffraction intensity profiles contained a number of characteristic peaks: typically, the diffraction series contained intense 6th, 9th and 11th peaks. These are also found to be characteristic of structures such as dry rat

tail tendon. It is therefore reasonable to simulate the electron density profile of parchment and deteriorated parchment based on a starting model that uses data derived from rat tail tendon molecular packing in the wet and dry state.

Model building The axial structure of tissues such as wet rat tail tendon can present a sequence of up to 140 meridional diffraction intensities. Recent studies have interpreted the electron density and demonstrate that the axial structure contains three key regions: the gap, overlap and telopeptides (see Fig. 3). The effects of drying and ageing may exist to different degrees in each of the three regions (above) due to the molecular topology and the molecular density in the pre-dried states. Diffraction of tendon samples in the wet state indicates the molecular structure at low angles to be dominated by strong first, third and fifth orders of intensities: this corresponds to the distinct gap overlap function. These features are absent from the dried samples, indicating that the gap overlap contrast density difference is weakened. This presumably relates to the effect of drying, where the water occupying the void of the gap region is removed. The collapse of the structure is also concomitant with the reduction of axial period length, indicating a concerted series of changes in the axial structure that occur on drying. The X-ray diffraction evidence also points to a larger degree of statistical disorder in the molecular organization within a fibril. This effect may also be compounded by deterioration of collagen in parchment samples, where peptide bond cleavage may induce even larger degrees of disorder.

The electron density distribution of the axial repeat was divided into a number of subsections: this allows the molecular structure to be simulated by producing electron density maps and judging the correlation with diffraction data. In an attempt to simulate the diffraction data, the first step was to alter the electron density difference between the gap and overlap regions.

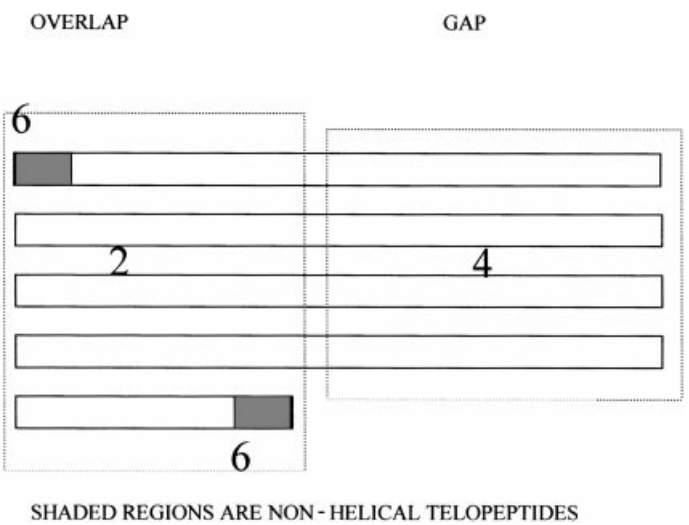

Figure 3 *The D periodic repeat of collagen and location of induced disorder. The axial unit cell of the collagen structure results from each helical molecule being staggered by 67 nm (or multiples of 67 nm) relative to each other. This gives a repeating structure that contains regions of high and low density. The ends of the molecule (telopeptides) are believed to have a more globular conformation. The estimated degree of disorder in a typically deteriorated sample is given as the isotropic displacement parameter value* $\langle u \rangle$*, in Ångstroms. The estimation is made by producing models of parchment structure where the static disorder induced by peptide cleavage and oxidative damage is simulated by isotropic random displacements of the electron density in the unit cell.*

The gap : overlap contrast difference is 0.8, which corresponds to four segments per axial unit cell in the gap region and five in the overlap region.

Results and applicability The static disorder is always found to be greatest in the telopeptide regions, and this may even point to different levels of occupancy in different D periodic structures. The isotropic displacement parameter r.m.s. values for the gap and overlap are comparable and in the region of 2–4 Ångstrom. Samples that exhibit weaker Bragg diffraction indicate that certain forms of deterioration relate to increased static disorder within the fibrils of a sample. A structural interpretation of the static disorder values in a D periodic unit is shown in Figure 3.

Principal components analysis of parchment diffraction An alternative method of data analysis was to examine the key features of collagen diffraction from a large pool of data. The process involves the determination of the deviations of each individual diffraction profile from an average diffraction profile. The differences are then converted into a series of eigenvalues and eigenfunctions, that are used to construct a series of orthogonal functions that deconstruct the diffraction profile. In the case of the data collected in this study, the functions correspond well with recognizable features within the diffraction profile, such as the background, changes in peak position and intensity and also the presence of the lipid ring that appears in a large number of parchment samples. The four main orthogonal functions are shown in Figure 4. Each diffraction profile consists of a discrete combination of the individual functions. The diffraction profiles can therefore be grouped together and the relationship between different component functions can be compared with other physical techniques of parchment analysis, such as DSC or shrinkage temperature.

Analysis of a manuscript in the style of Central Mexican pictorial writing (first part of 16th century)

This example highlights the use of X-ray diffraction to provide information that is not readily obtained from other sources and also emphasizes the ability to distinguish between different textures or composites within a very small sample. The sample was provided by Maria Gaida from the Berlin Ethnographical Museum (Ethnologisches Museum Staatliche Museen zu Berlin Preußischer Kulturbesitz). It is believed to be post-1492, but the provenance is not clear.

The pigments used to decorate the sample were not fully analysed and the suitability of X-ray microdiffraction to examine the powder diffraction pattern of the different layers of pigment was to be assessed. The sample contained a substrate (a cellulosic material) followed by a dark red layer that contained iron and was overlaid by a thick red layer of minium with a dark red layer at the surface—a possible degradation product of minium (see Fig. 5).

The sample examined was prepared for analysis by Jan Wouters of the Royal Institute for Artistic Heritage, Brussels, by a microdrilling technique in which a 200 μm diameter bore of the sample was taken and then sectioned for a variety of optical and diffraction analyses. Microcylinder sampling of historic samples is seen as a method with great future potential, as sample analysis becomes more sensitive and more sophisticated.

The bore sample was embedded in polyester resin and then subsequent microtoming was used to produce cross-sections with a thickness of 10 μm. The elimination of extending polyester with a scalpel was performed to reduce curling of the sample prior to viewing the section on a glass microscope slide. A small drop of Canada balsam was put close to the section, and the section was flattened and soaked with Canada balsam by covering it with a thin plastic cover

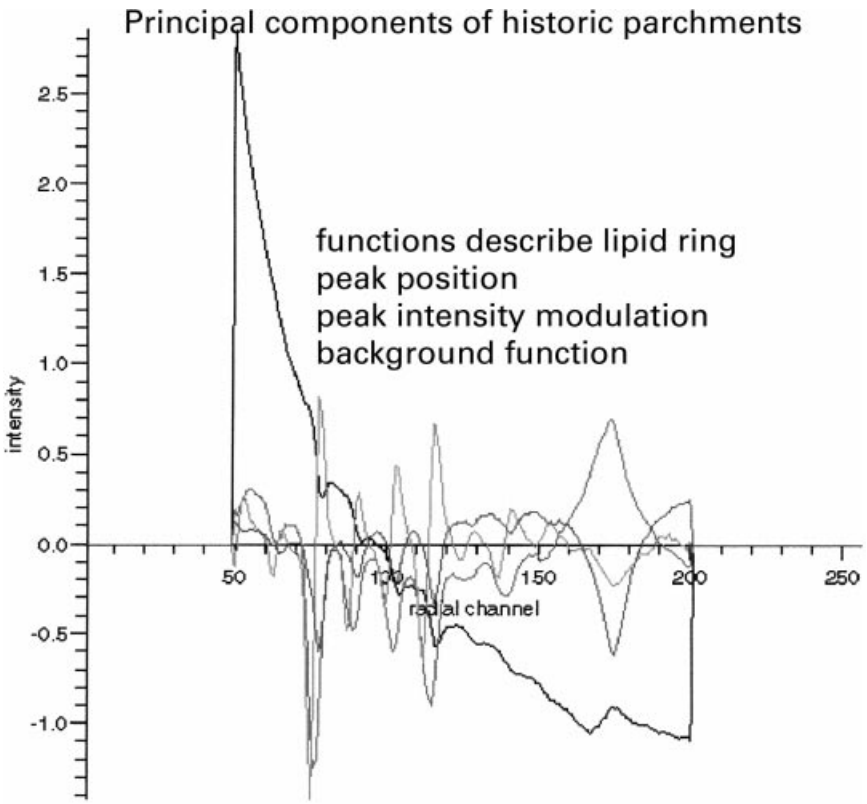

Figure 4 *Principal components analysis of parchment. A series of orthogonal functions describe the radially averaged diffraction patterns of historic parchments. The first five functions account for 98% of the diffraction data (for reasons of clarity, only the first four are shown here). The functions account for different features found within the diffraction pattern. The first order function mainly accounts for the diffuse scattering function, while others characterize the diffraction peak intensity and position, as well as the presence of lipids. By analysing the fractional contribution of different functions in various historic parchments, it is possible to relate the changes in the diffraction pattern to the process of deterioration. ———, First component; — — —, second component; . . . . ., third component; - - - - -, fourth component.*

slide. Optical microscopy, using a halogen light in transmission and reflection modes, shows the different features.

The sample provided for X-ray diffraction was barely visible with the naked eye and is shown in Figure 5: it was suspended between two pinholes and analysed with a $1 \times 5\ \mu$m beam of energy 20 keV at beamline ID22 at ESRF, Grenoble, by M. Drakopoulos, A. Snigirev and I Snigireva. The diffraction patterns from four regions of the sample were recorded using a medium to high-angle diffraction geometry as compared to the studies of bone mineral (see the next example). The results of the diffraction study can be seen in Figure 6. The microdiffraction technique was successful on two accounts. First, distinct X-ray diffraction patterns of each region were obtained, indicating the great usefulness of this technique to distinguish textures at the micron scale. Second, although $10\ \mu$m thick, the sample was able to produce scattering of sufficient intensity in the minute timescale to make the technique useful for the rapid analysis of historic or archaeological samples.

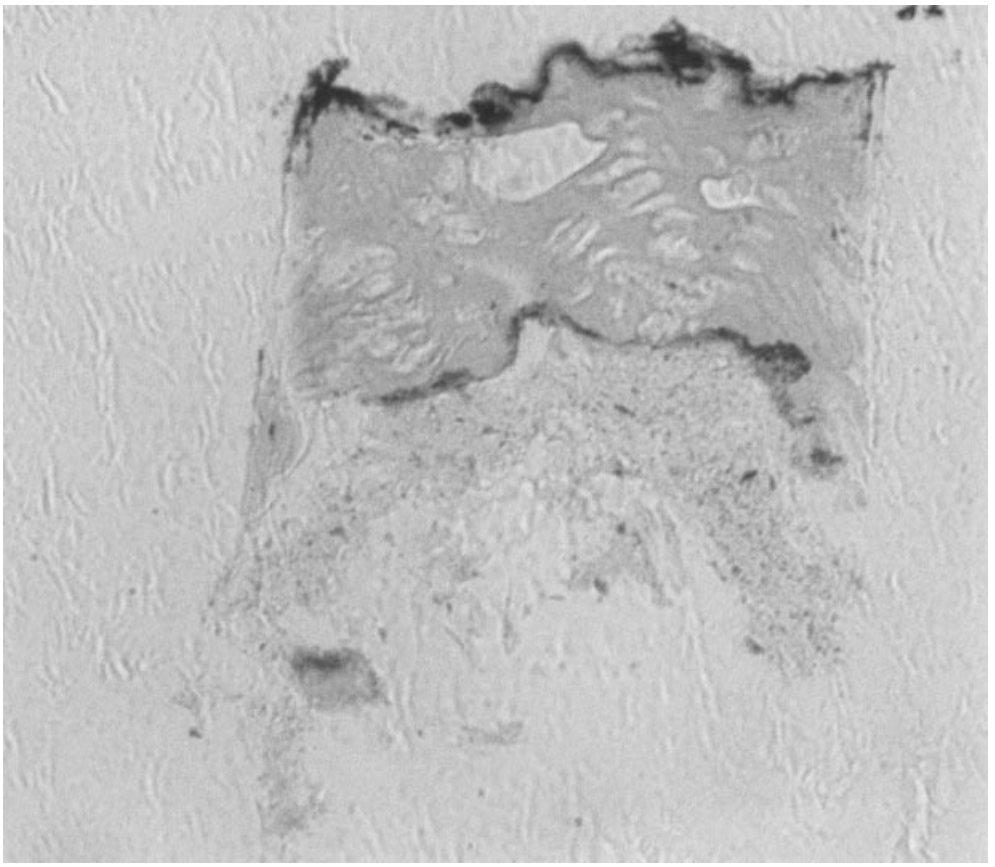

Figure 5 *A 10 μm section of a microdrilled* c. *16th century Central Mexico style pictograph. The following strata are shown (from base to top): the substrate (a cellulosic material); a dark red layer, containing iron, possibly α-hematite; a thick red layer of minium (Pb_3O_4); and a dark red layer on top, possibly a degradation product of minium (PbO_2).*

The analysis of the data is still in progress, and the ability to identify the mineral phases has been hampered by the microfocus being so small that only a small number of mineral crystallites were diffracting at one time. This means that the diffraction occurred as discrete spots rather than a series of Deybe Scherrer powder rings, used in conventional powder diffraction analysis. It is hoped, however, that the reflections observed can be used to discriminate between possible lead-based mineral forms and also allow the oxide form of the iron salt to be identified.

Diffraction of archaeological bone samples and the application of microdiffraction

The archaeological degeneration of bone involves a number of processes that indicate specific forms of geological or microbial degeneration (Hedges and Millard 1995). The most important of these are diagenesis involving Ostwald ripening and pore formation. These processes involve the remodelling of the mineral and collagen matrix of bone: however, the exact nature of the rearrangements is poorly defined. *In vivo*, bone consists of a matrix of collagen fibrils that provides a framework for calcium hydroxyapatite organization. The hydroxyapatite is found as discrete needle or plate-like crystal structures, with a mean thickness of 2–3 nm.

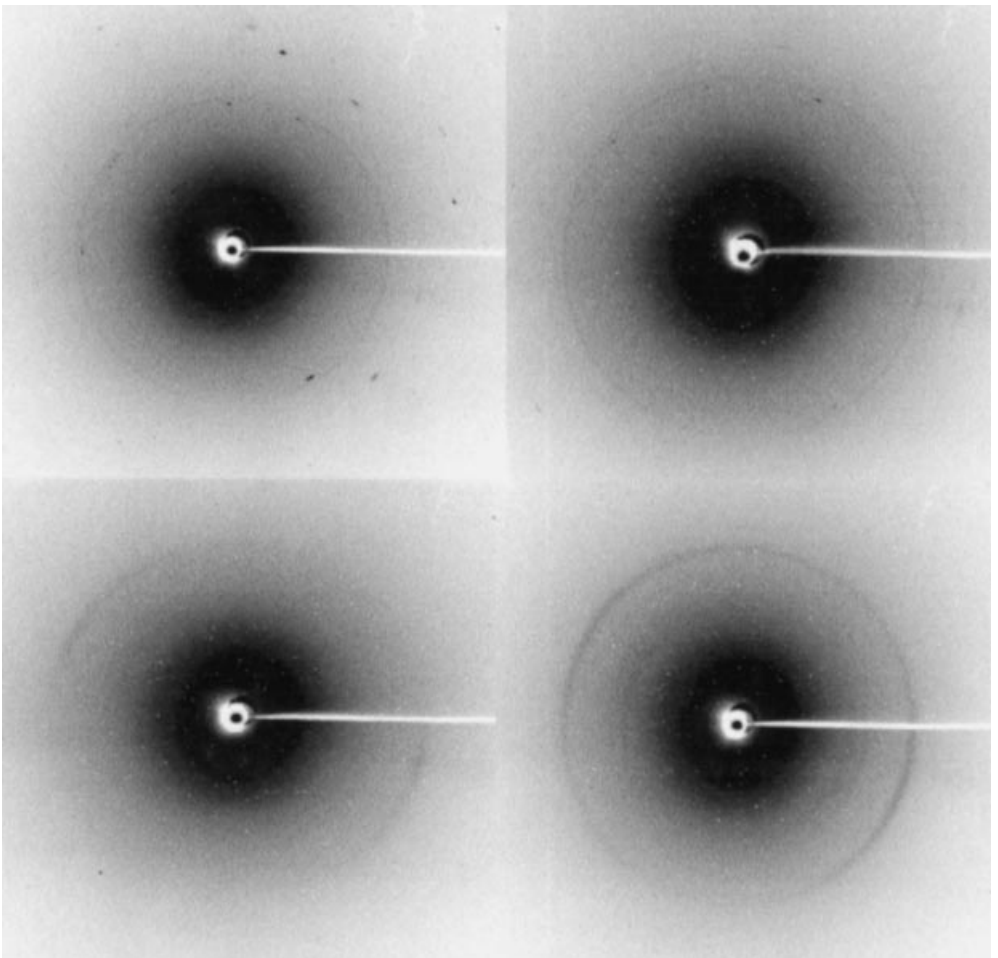

Figure 6 *X-ray diffraction images from the different layers of the microdrilled sample, obtained at beamline ID22 of ESRF, Geneva, by M. Drakopoulos; the diffraction patterns change as different textures are analysed. The smooth diffraction rings of amorphous cellulose-based material are contrasted with the sharp diffraction peaks from the microcrystalline texture of the mineral used in the pigment. Top left, the central region of the red pigment; top right, the suspected iron-based layer; bottom left, the upper cellulose and possible binding medium; bottom right, the central region of the cellulose substratum.*

The effects of *post mortem* changes such as cremation, combined with archaeological changes, result in deviations from the mean crystal thickness, often producing larger crystals. However, to date the exact character of the changes is poorly defined. Some processes, such as cooking or cremation, are expected to have a more global effect on crystal habit, whereas bacterial or hydrological changes are expected to produce focal changes in bone character at the micron length scale. In order to develop an understanding of properties such as differential diagenetic durability between and within the heterogeneous architecture of bones, it is essential to provide information about changes in crystal habit, orientation and the statistical distribution of mean thickness. This will lead to an understanding of the archaeological remodelling that occurs at the molecular levels and manifests itself at the level of macroscopic bone integrity.

Small-angle X-ray scattering has proved to be very successful in determining the statistical habit of mineral in tissues such as bone (Camacho *et al.* 1999; Rinnerthaler *et al.* 1999). The technique measures the scattering from the inorganic crystals within a bone that is bathed by an X-ray beam. The shape of the scattered X-ray profile at very low angles allows parameters such as the average crystal thickness and crystal shape to be determined. Further analysis of the data also allows the statistical spread of the crystalline form to be estimated, such as in the case of osteoporotic bone (Fratzl *et al.* 1996). The technique is less subjective than electron microscopy and also does not rely on factors such as the degree of crystallinity, which hamper comparisons of crystal size between samples made by high-angle X-ray diffraction.

Recent major developments in microfocus technology for X-ray scattering, at the European Synchrotron Research Facility (ESRF, Grenoble; Snigirev *et al.* 1996), allow the analysis of changes in the texture of very small regions of bone where focal changes in mineral habit may have occurred. This provides a unique opportunity to study local changes in the crystal morphology and size distribution within archaeological bone. The ESRF also has facilities for microfluorescence analysis, that can monitor trace element levels simultaneously with scattering experiments. The technique is non-destructive and allows parallel studies on the same archaeological bone sample; therefore, the technique allows light microscopy to identify regions of interest that can subsequently be examined by X-ray scattering.

X-ray scattering of archaeological bone A study to examine the changes in crystal parameters within archaeological bone was performed at the University of Leoben, Austria, using a conventional laboratory X-ray source (NanoStar, with a rotating anode X-ray generator from BRUKER AXS, Karlsruhe). The operational details were as follows: diffracting wavelength $Cu{-}K_{\alpha}$ (0.154 nm), 40 kV, 40 mA, with a 0.2×0.2 mm focal spot. The monochromator and beam defining unit were cross-coupled Göbel Mirrors and a 0.1 mm beam-defining pinhole. The resultant beam size at the sample was approximately 0.2 mm, with a sample-to-detector distance of 680 mm. The detector was a Hi-Star (BRUKER AXS) 2-D proportional counter.

Bone samples were measured over a number of different regions, and the data were collected and analysed with in-house software. This allowed the radially averaged scattering profile to be displayed, and the shape of the crystallites could be inferred from this (see Fig. 7). A crystal thickness parameter T was estimated from the data in accordance with methodologies described by Fratzl *et al.* (1996).

A well preserved wolf humerus (94% of the original collagen) from Carsington Pasture Cave (Chamberlain 1999) was found to contain crystals of a size and shape parameters commensurate with those of bone crystals found *in vivo* (3–4 nm). In contrast, the pelvis from a small pig (36% collagen) displayed variable crystal size; in one region the crystal thickness parameter had risen to at least 5.1 nm, yet in another region of the same bone section, the value for T was lower (4.1 nm) and the habit of the crystal was easier to identify as being plate-like. This (domestic) pig bone was from the same archaeological level, implying perhaps that the bone had been introduced into the cave after having suffered some diagenetic alteration. The ability of the technique to determine crystal size and shape quickly and reliably lends itself to the analysis of archaeological bone.

X-ray microfocus of calcified samples We have conducted experiments that show the feasibility of X-ray scattering, providing significant results from bone and calcified tendon samples of $1-10\,\mu$m thickness at ESRF. The beam used was $1 \times 5\,\mu$m at the sample and allowed the changes in mineralization within regions of tissues from contemporary sources to be determined. The samples used were of turkey leg tendon, since this has provided biologists with a highly structured calcified tissue standard.

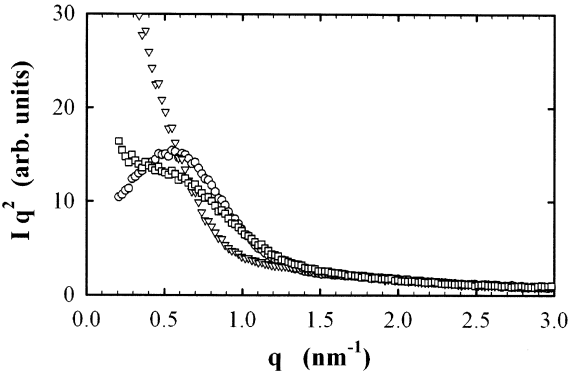

Figure 7 The *radially averaged X-ray scattering profiles of the archaeological and cooked bones. The data are plotted as the intensity multiplied by q^2, where q is the scattering angle multiplied by $4\pi/\lambda$ (the wavelength). This is known as a Kratky plot. This method of plotting is especially useful in determining the crystal thickness parameter T, and also gives an indication of the shape of the mineral crystallites. Bones that have undergone comprehensive diagenetic remodelling (triangles) are observed to have very large (and probably highly variable) crystal sizes, as judged by the large negative slope at low q values. Bones from the same site that still show relatively little diagenetic alteration are demonstrated by the squares. The shape of the curve is typical of plate-like crystals, and the thickness parameter is commensurate with the sizes found* in vivo*. A third example (a scattering profile, shown as circles) typifies scattering from needle-like apatite crystals of a cooked contemporary bone.*

Using the ID22 microfocus beamline in small-angle scattering mode, we were able to measure the changes in scattering from the nascent edge of calcification in tendon from 3 μm thick sections at 5 μm intervals. The angular dependence of scattering was used to determine the crystal thickness parameter *T* and also to estimate the shape of the first mineral crystals that could be detected from the growing edge of the mineral over the first 30 μm of calcified turkey leg tendon. The results indicate that the overall thickness of the hydroxyapatite crystals was related to the overall age of the bird; more so than their position from the edge of mineralization. The shape of the detectable crystallites also tended to be similar over the distance examined, indicating that the bone growth is due to the thickening and extension of plate-like structures, as opposed to the fusion of needle-like structures to form plates.

Future studies The ability spatially to resolve the variation in crystal size and habit has implications for the procedure of 'sequential washing'. This is an approach designed to remove diagenetic material from bone, proposed by Sillen and Sealy (1995), and used extensively in archaeological and palaeontological research. In order to explore this further, degraded and fresh bone will be subjected in the laboratory to the solubility profile procedures recommended by Sillen and Sealy, and the crystallographic alteration directly monitored by SAXS. Biologically driven processes may be confined to regions of focal destruction, whereas chemically driven processes may yield histologically well preserved regions. Therefore development of the micron-sized beam facilities will provide a unique opportunity for an advancement in the understanding of bone durability and diagenesis.

CONCLUSIONS

From the foregoing examples, the scope and potential of X-ray diffraction and scattering studies of historical and archaeological based materials can be seen. The two main thrusts are the ability of the technique to characterize the molecular packing, surface area and even, in the case of

minerals, the composition of a sample. The advent of microfocus technology means that textures within a single sample can be examined in this way. The processes of deterioration and remodelling that occur within historical and archaeological samples can also be determined; as can the more pressing effects of urban air pollution. The scope for future studies is only just emerging.

ACKNOWLEDGEMENTS

I would like to thank Linton Brown for the preparation of thin sections of bone at Stirling as well as Professor A. T. Chamberlain of the University of Sheffield for the preparation of thin archaeological sections. Helpful discussion of the analysis of archaeological bone was provided by Professor Mark Pollard of the University of Bradford. We would also like to thank all staff at ESRF, especially Irina Snigireva, and also Gunter Grossmann at beamline 2.1 of the CCLRC Daresbury synchrotron. This work was funded in part by NERC Grant GR8/5019.

REFERENCES

Camacho, N. P., Rinnerthaler, S., Paschalis, E. P., Mendelsohn, R., Boseky, A. L., and Fratzl, P., 1999, Complementary information on bone ultrastructure from small angle scattering and Fourier transform infrared microspectroscopy, *Bone*, **25**, 287–93.

Chamberlain, A. T., 1999, Carsington Pasture Cave, Brassington, Derbyshire: a prehistoric burial Site, http://www.shef.ac.uk/~capra/1/carsing.html

Fraser, R. D. B., and MacRae, T. P., 1973, *Conformation in fibrous proteins*, Academic Press, New York.

Fratzl, P., Schreiber, S., and Klaushofer, K., 1996, Bone mineralisation as studied by small angle scattering, *Connective Tissue Research*, **34**, 247–54.

Guinier, A., 1963, *X-ray diffraction in crystals, imperfect crystals, and amorphous bodies*, W. H. Freeman, San Francisco.

Hedges, R. E. M., and Millard, A. R., 1995, Bones and groundwater: towards the modelling of diagenetic processes, *Journal of Archaeological Science*, **22**, 155–65.

Hukins, D. W. L., 1981, *X-ray diffraction by disordered and ordered systems*, Pergamon Press, Oxford.

Lewis, R., 1994, Multiwire gas proportional counters: decrepit antiques or classic performers? *Journal of Synchrotron Radiation*, **1**, 43–53.

Perkins, S. J., Ashton, A. W., Bohem, M. K., and Chamberlain, D., 1998, Molecular structures from low angle X-ray and neutron scattering studies, *International Journal of Biological Macromolecules*, **22**, 1–16.

Rinnerthaler, S., and Fratzl, P., 1999, Small angle scattering measurements of human bone sections, *Calcified Tissue International*, **64**, 422–9.

Sillen, A., and Sealy, J., 1995, Diagenesis of strontium in fossil bone: a reconsideration of Nelson *et al.* (1986), *Journal of Archaeological Science*, **22**, 313–20.

Snigirev, A., Kohn, V., Snigireva, I., and Aristova, E., 1996, A compound reflective lens for focussing high energy X-rays, *Nature*, **384**, 49–51.

Towns-Andrews, E., Berry, A., Bordas, J., Mant, P. K., Murray, K., Roberts, K., Sumner, I., Worgan, J. S., and Lewis, R., 1989, Time-resolved X-ray diffraction station: X-ray optics, detectors, and data acquisition. *Review of Scientific Instruments*, **60**, 2346–9.

Vainshtein, B. K., 1966, *Diffraction of X-rays by chain molecules*, Elsevier, London.

Wess, T. J., Hammersley, A. P., Wess, L., and Miller, A., 1998, Molecular packing of type I collagen in tendon, *Journal of Molecular Biology*, **275**, 255–67.